

# Effect of Hypoxia on the Function of the Human Serotonin<sub>1A</sub> Receptor

Aritri Dutta, Parijat Sarkar, Sandeep Shrivastava, and Amitabha Chattopadhyay\*

Cite This: *ACS Chem. Neurosci.* 2022, 13, 1456–1466

Read Online

ACCESS |



Metrics &amp; More



Article Recommendations



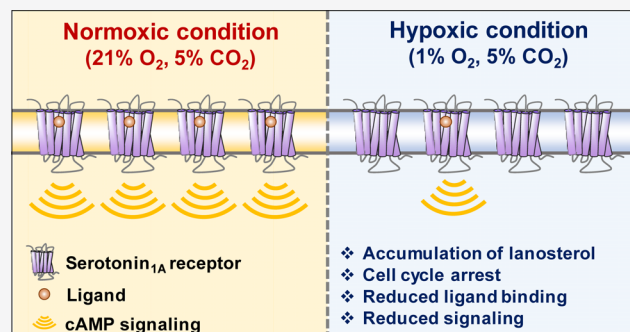
Supporting Information

**ABSTRACT:** Cellular hypoxia causes numerous pathophysiological conditions associated with the disruption of oxygen homeostasis. Under oxygen-deficient conditions, cells adapt by controlling the cellular functions to facilitate the judicious use of available oxygen, such as cessation of cell growth and proliferation. In higher eukaryotes, the process of cholesterol biosynthesis is intimately coupled to the availability of oxygen, where the synthesis of one molecule of cholesterol requires 11 molecules of O<sub>2</sub>. Cholesterol is an essential component of higher eukaryotic membranes and is crucial for the physiological functions of several membrane proteins and receptors. The serotonin<sub>1A</sub> receptor, an important neurotransmitter G protein-coupled receptor associated with cognition and memory, has previously been shown to depend on cholesterol for its signaling and function. In this work, in order to explore the interdependence of oxygen levels, cholesterol biosynthesis, and the function of the serotonin<sub>1A</sub> receptor, we developed a cellular hypoxia model to explore the function of the human serotonin<sub>1A</sub> receptor heterologously expressed in Chinese hamster ovary cells. We observed cell cycle arrest at G1/S phase and the accumulation of lanosterol in cell membranes under hypoxic conditions, thereby validating our cellular model. Interestingly, we observed a significant reduction in ligand binding and disruption of downstream cAMP signaling of the serotonin<sub>1A</sub> receptor under hypoxic conditions. To the best of our knowledge, our results represent the first report linking the function of the serotonin<sub>1A</sub> receptor with hypoxia. From a broader perspective, these results contribute to our overall understanding of the molecular basis underlying neurological conditions often associated with hypoxia-induced brain dysfunction.

**KEYWORDS:** hypoxia, cholesterol, lanosterol, cell cycle, serotonin<sub>1A</sub> receptor, cAMP

## INTRODUCTION

Oxygen (O<sub>2</sub>)-producing cyanobacteria changed the course of natural evolution nearly 2.5 billion years ago.<sup>1</sup> With increasing O<sub>2</sub> levels in the atmosphere (finally reaching ~21%), evolution of more complex aerobic organisms was initiated,<sup>2</sup> and O<sub>2</sub> became integral to various biochemical pathways.<sup>3</sup> The sterol biosynthetic pathway became oxygen-dependent, and in due course of evolution, it developed into the current pathway.<sup>4,5</sup> The concept of hypoxia or oxygen deficiency in cells emerged as oxygen became crucial for cellular survival.<sup>6</sup> Every tissue has an ideal oxygen pressure ( $p_{O_2}$ ) that maintains tissue metabolism which is regulated by a number of extrinsic and intrinsic factors.<sup>7,8</sup> A continued exposure to hypoxia results in pathophysiology associated with heart disease, cancer, cerebrovascular disease, and chronic lung disease.<sup>9</sup> Cerebral hypoxia is caused by impaired blood flow as a result of cerebral or myocardial ischemia<sup>7</sup> and exposure to diminished oxygen pressure in high altitude.<sup>10</sup> Interestingly, hypoxia induced by Covid-19 (termed “happy hypoxia”) has been recently reported to pose a novel challenge to physicians treating Covid patients.<sup>11,12</sup> Although human brain comprises only 2%



of the body weight, it consumes 20% of oxygen supply from our body in spite of its relatively small size.<sup>13</sup> As a consequence, prolonged hypoxia cannot be sustained by the brain, leading to seizures, coma, and even death.<sup>7,14</sup>

There are inbuilt oxygen sensors at the cellular level capable of detecting oxygen deficiency and directing cells toward either an adaptive response or a stress response, while balancing oxygen homeostasis.<sup>15</sup> These responses could vary, depending on whether the hypoxia is severe (0.01% O<sub>2</sub>), causing the inhibition of nucleotide synthesis, or moderate (~1% O<sub>2</sub>), causing numerous biological reactions to deviate from their normal functions.<sup>16</sup> Cellular hypoxia<sup>17</sup> alters cell proliferation in two distinct ways, either by apoptosis or by growth arrest.<sup>18</sup> An imbalance in cellular O<sub>2</sub> homeostasis has implications in

Received: March 23, 2022

Accepted: April 13, 2022

Published: April 25, 2022



cellular lipid metabolism in general<sup>19</sup> and cholesterol metabolism in particular.<sup>4</sup> The synthesis of one molecule of cholesterol requires 11 molecules of O<sub>2</sub><sup>20</sup> (see Figure 1), and

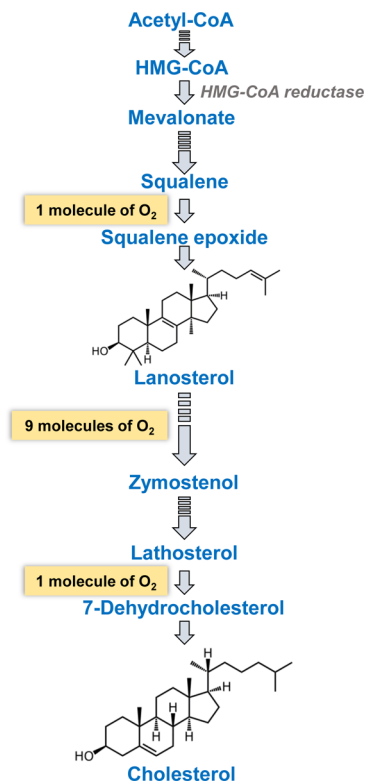


**Figure 1.** Evolutionary link between oxygen and cholesterol biosynthetic pathway. Biosynthesis of cholesterol begins with acetyl-CoA that feeds into the mevalonate pathway to generate lanosterol. Lanosterol-to-cholesterol conversion includes multiple steps. This oxygen-intensive conversion utilizes nine molecules of oxygen to remove methyl groups at 4 $\alpha$ , 4 $\beta$ , and 14 $\alpha$  in lanosterol to convert to zymostenol. The final oxygen-requiring step in cholesterol synthesis consumes one molecule of oxygen, resulting in the reduction of lathosterol to 7-dehydrocholesterol. Lack of oxygen slows down lanosterol conversion, leading to its accumulation in cells, ultimately disrupting the cholesterol biosynthetic pathway. The solid and dashed arrows represent single and multistep reactions. See text for more details.

the stepwise progression from squalene, lanosterol demethylation, and finally to cholesterol is believed to be in agreement with the increasing oxygen concentration along the evolutionary timescale.<sup>21</sup> Lack of cellular oxygen required for removing the methyl groups from lanosterol at 4 $\alpha$ , 4 $\beta$ , and 14 $\alpha$  positions slows down the intermediate steps from lanosterol to cholesterol synthesis and leads to the accumulation of lanosterol and its metabolites in cells.<sup>22</sup> The methylated sterols accumulated in cell membranes act as endogenous regulators and trigger the direct rapid ubiquitin-mediated degradation of 3-hydroxy-3-methyl-glutaryl-CoA reductase (HMG-CoA reductase),<sup>22,23</sup> a rate-limiting enzyme in the cholesterol biosynthetic pathway.

Cholesterol is a crucial lipid in higher eukaryotic cell membranes as it regulates organization, dynamics, function, and sorting in cells.<sup>24,25</sup> Importantly, cholesterol is evolutionarily superior in terms of carrying out essential membrane functions relative to other precursor sterols.<sup>21,26</sup> The non-random distribution of cholesterol in physiologically significant

domains in membranes is a crucial determinant in supporting the membrane structure and function.<sup>27</sup> On the other hand, lanosterol, with three methyl groups protruding from its planar structure, exhibits a rough structure, rendering it functionally unfit as a membrane sterol.<sup>4,28</sup> Cholesterol biosynthesis is known to play a crucial role in growth and division in mammalian cells.<sup>29</sup> Notably, cholesterol is differentially synthesized during the different phases of the cell cycle,<sup>30,31</sup> and the presence of cholesterol is indispensable to progress from G1 to S phase.<sup>30</sup>

G protein-coupled receptors (GPCRs) are the largest class of integral membrane proteins that respond to a variety of external stimuli, ranging from photons to small molecules, and act as important drug targets.<sup>32,33</sup> The serotonin<sub>1A</sub> receptor, an extensively studied neurotransmitter receptor in the GPCR superfamily,<sup>34–37</sup> is associated with anxiety, stress, learning deficiency, cognition, and mood disorders<sup>38</sup> and serves as an important drug target for numerous psychiatric disorders.<sup>39–41</sup> Interestingly, the level of the neurotransmitter serotonin, an endogenous ligand for the serotonin<sub>1A</sub> receptor, has been reported to be altered under hypoxic conditions.<sup>42–44</sup> The expression of the serotonin transporter, which removes serotonin from the synaptic cleft to the presynaptic neuron, is known to be affected by hypoxia.<sup>43,45,46</sup> In addition, the levels of serotonin<sub>1B</sub> and serotonin<sub>2B</sub> receptors have been shown to be modulated by hypoxia.<sup>43</sup> Yet, the effect of hypoxia on the function of the serotonin<sub>1A</sub> receptor remains elusive. Previous works from our laboratory using a judicious combination of biophysical, biochemical, cell biological, and molecular dynamics simulation approaches have established that membrane cholesterol plays a crucial role in ligand binding, G-protein coupling, signaling, and oligomerization of the serotonin<sub>1A</sub> receptor.<sup>37,47–52</sup> In addition, we have recently showed that the endocytic pathway and intracellular trafficking of the serotonin<sub>1A</sub> receptor are modulated by cholesterol,<sup>53,54</sup> and subcellular localization of the receptor is altered in Smith–Lemli–Opitz syndrome (SLOS),<sup>55</sup> a congenital and developmental malformation syndrome associated with defective cholesterol biosynthesis.

In order to elucidate the interdependence of oxygen levels, cholesterol biosynthesis, and the function of the human serotonin<sub>1A</sub> receptor, in this work, we explored the function of the serotonin<sub>1A</sub> receptor under hypoxic conditions. As hypoxia is associated with reduced cognition, depression, and anxiety,<sup>56</sup> exploring the function of neuronal receptors under this condition assumes significance. In this work, we developed a cellular hypoxia (~1% O<sub>2</sub>) model and explored the effect of long-term hypoxia in Chinese hamster ovary (CHO-K1) cells stably expressing the human serotonin<sub>1A</sub> receptor. We confirmed the validity of the cellular model by estimating the accumulation of lanosterol, a well-known sterol marker of hypoxia.<sup>22,23</sup> We further show here that ligand binding and cellular signaling by the serotonin<sub>1A</sub> receptor get compromised during prolonged exposure to hypoxia. To the best of our knowledge, our results represent the first report linking the function of the serotonin<sub>1A</sub> receptor with hypoxia. From a broader perspective, these results contribute to our overall understanding of the molecular basis underlying the neurological conditions during hypoxia and could provide crucial insights into the malfunctioning of receptors in diseases (such as cancer) characterized by hypoxic conditions.

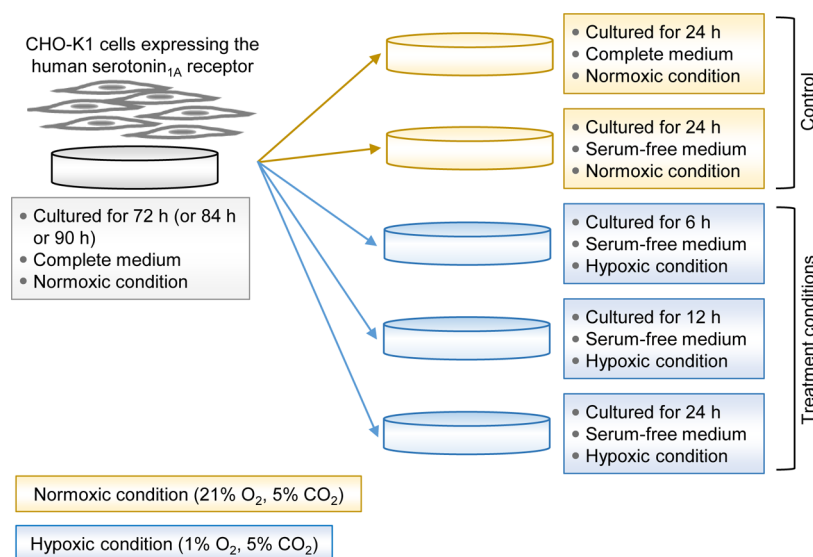


**Figure 2.** Schematic representation of the experimental design for generating the cellular hypoxia model. CHO-K1 cells stably expressing the serotonin<sub>1A</sub> receptor were cultured for 72 h (or 84 h or 90 h) in complete culture medium (medium containing fetal calf serum) under normoxic conditions (21% O<sub>2</sub> and 5% CO<sub>2</sub>) at 37 °C in a humidified incubator. The cells were subsequently subjected to various treatment conditions. Three sets of cells were shifted to hypoxic conditions (1% O<sub>2</sub> and 5% CO<sub>2</sub>) at 37 °C and were cultured in serum-free culture medium for 6, 12, or 24 h in a humidified incubator where the oxygen concentration could be regulated. Two sets of control cells were cultured for 24 h in complete or serum-free culture medium under normoxic conditions (21% O<sub>2</sub> and 5% CO<sub>2</sub>) at 37 °C in a humidified incubator. See [Methods](#) and [Figure S1](#) for more details.

## RESULTS

**Generating a Cellular Hypoxia Model.** Cells grown *in vitro* are usually maintained at an optimum oxygen concentration for their growth in normal atmospheric oxygen pressure in a regular humidified incubator (21% O<sub>2</sub> and 5% CO<sub>2</sub>). To mimic hypoxic conditions, we developed a cellular hypoxia model ([Figures 2](#) and [S1](#)) and cultured cells in a humidified incubator where the oxygen concentration could be regulated using excess of nitrogen. We cultured cells using 1% O<sub>2</sub> and 5% CO<sub>2</sub> for 6, 12, and 24 h to mimic hypoxia.<sup>17,22</sup> We utilized CHO-K1 cells stably expressing the human serotonin<sub>1A</sub> receptor with (or without) an enhanced yellow fluorescent protein (EYFP) tag at its C-terminal (denoted as CHO-5-HT<sub>1A</sub>R-EYFP and CHO-5-HT<sub>1A</sub>R, respectively) for this purpose. We previously showed that the human serotonin<sub>1A</sub> receptor stably expressed in CHO-K1 cells retains all the characteristics of the native receptor expressed in hippocampus in terms of ligand binding, G-protein coupling, and signaling, even when labeled with EYFP.<sup>57,58</sup> In order to avoid the uptake of exogenous cholesterol from the serum present in a complete culture medium, we cultured cells in a serum-free medium under hypoxic conditions.<sup>59</sup> To rule out any possible effect of the serum-free medium itself, control cells were grown in both complete and serum-free culture media under normoxic conditions for 24 h (see [Figures 2](#) and [S1](#)).

In the cholesterol biosynthetic pathway, demethylation of lanosterol and subsequent conversion to cholesterol consume 10 molecules of oxygen ([Figure 1](#)). The hallmark of cellular hypoxia is slow lanosterol demethylation and subsequent accumulation of lanosterol in the cells due to oxygen deficiency.<sup>22,23</sup> In order to validate the cellular model of hypoxia, we checked the accumulation of lanosterol under hypoxic conditions. For this, lipid extracts were prepared from cell membranes, and lipids were separated by thin-layer chromatography. [Figure 3a](#) shows a representative thin-layer

chromatogram showing the lipid composition of cells under various conditions. As shown in the figure, we did not observe any band corresponding to lanosterol under control conditions. However, bands corresponding to lanosterol could be visualized after 12 h of exposure to hypoxia, and a considerable amount of lanosterol could be detected when cells were grown under hypoxic conditions for 24 h. Densitometric analysis of the TLC bands showed lanosterol/total sterol ratio of 0.01 and 0.05 in cells exposed to hypoxic condition for 12 and 24 h, respectively ([Figure 3b](#)). These results validate our cellular model for hypoxia.

**Membrane Cholesterol Content Does Not Change in Cells under Hypoxia.** As described above, we observed a distinct accumulation of lanosterol under hypoxic conditions. However, no apparent change in cholesterol level was found under hypoxia when analyzed using densitometric analysis of the chromatogram ([Figure 3b](#)). We therefore used a more sensitive fluorometry-based Amplex Red assay for the quantification of cholesterol under these conditions.<sup>60</sup> Importantly, our control experiments showed that the presence of lanosterol does not interfere with this assay (data not shown). [Figure 3c](#) shows the cholesterol content in cells cultured under normoxic and hypoxic conditions. As shown in the figure, we did not observe any significant change in the cholesterol content in all cases.

**Cell Viability under Hypoxic Conditions.** Low oxygen could affect cellular functions, and cells are known to activate apoptosis under prolonged hypoxic treatment.<sup>61</sup> In addition, the accumulation of lanosterol leads to toxicity<sup>62</sup> and is associated with its inability to maintain the normal physiological properties of cell membranes essential to carry out crucial functions.<sup>25,63</sup> We therefore chose the duration of hypoxic treatment carefully to ensure that cell viability was not compromised in our experimental conditions. Apoptosis was measured utilizing a flow cytometry-based assay using FITC-Annexin V and propidium iodide (PI). Whereas apoptosis is

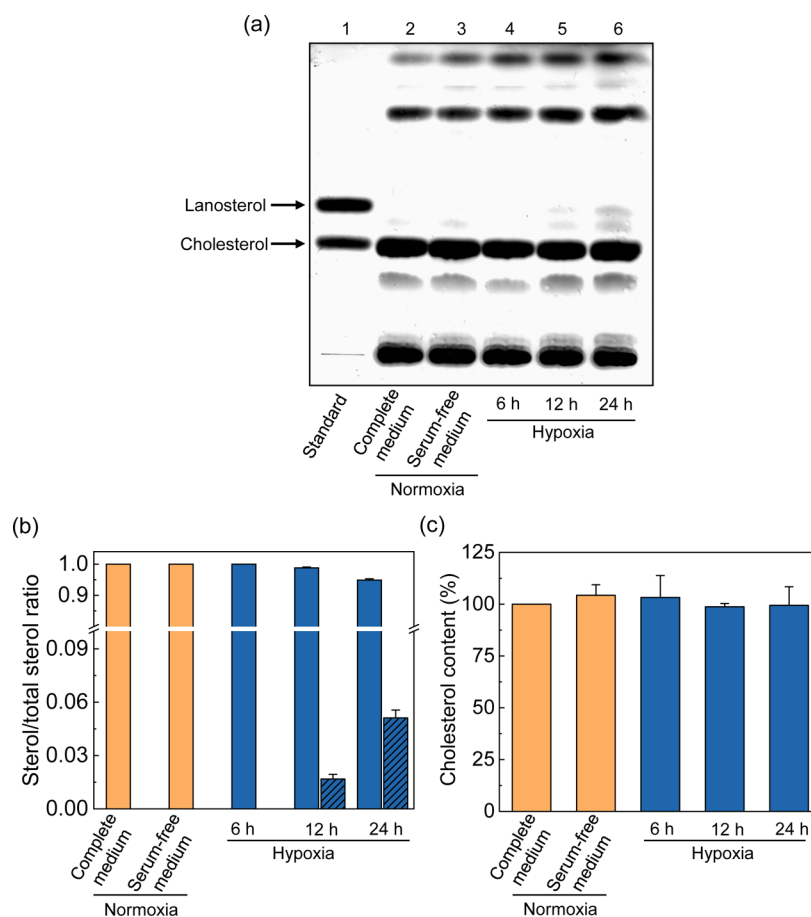


**Figure 3.** Representative thin-layer chromatogram of lipid extracts under hypoxia. (a) Lanosterol accumulation in cells cultured under hypoxic conditions for 6 h (lane 4), 12 h (lane 5), and 24 h (lane 6) was monitored by thin-layer chromatography. Lipids extracted from control cells grown under normoxic conditions are shown in lanes 2 and 3. The arrows represent the positions of cholesterol and lanosterol on the thin-layer chromatogram identified using standards in lane 1. Distinct lanosterol accumulation was observed at 12 h (lane 5) and 24 h (lane 6). (b) Quantitation of cholesterol/total sterol ratio (orange and blue solid bars) and lanosterol/total sterol ratio (hatched blue bars) was performed using densitometric analysis. Values are expressed as relative sterol content normalized to total sterol from the corresponding samples in each case. Data represent means  $\pm$  SE from three independent experiments. (c) Cholesterol content in membranes of cells grown under normoxic and hypoxic conditions measured using the Amplex Red assay. No significant change in cholesterol content was observed in cells under hypoxic conditions (blue bars) relative to control cells (orange bars). Values are expressed as percentages of cholesterol content normalized to control cells grown in complete medium. Data represent means  $\pm$  SE of at least three independent experiments. See [Methods](#) for more details.

characterized by phosphatidylserine (PS) externalization on the cell surface<sup>64</sup> and significant membrane defects in later phases, necrosis is characterized by significant membrane defects that do not involve externalization of PS. Externalized PS binds to Annexin,<sup>65</sup> and the fluorescence from the tagged FITC is quantitated to determine the extent of apoptosis. On the other hand, PI intercalates with nucleic acids, and its fluorescence allows discrimination between the late apoptotic phase and necrosis. [Figure S2](#) shows the representative flow cytometric dot plots with four distinct quadrants marked as viable cells (Annexin-FITC and PI-negative cells), early apoptosis (only Annexin-FITC-positive cells), late apoptosis (Annexin-FITC and PI double-positive cells), and necrosis (only PI-positive cells). We observed that  $\sim$ 99% cells across all treatment conditions did not exhibit apoptosis and were comparable to the control cells grown in complete media.

#### Cell Cycle Progression under Hypoxic Conditions.

Hypoxia is known to induce cell cycle arrest at the G1/S interphase.<sup>18</sup> In order to validate the effect of hypoxia on the cell cycle progression in our cellular model, we utilized a flow cytometry-based assay to quantitate the number of cells in

various phases of the cell cycle. The phases of cell cycle could be identified on the basis of the changes in the cellular DNA content in a population of cells using flow cytometry acquired upon PI labeling. In order to estimate the effect of hypoxia, the distribution of cells (*i.e.*, number of cells in G1, S, G2/M, and sub-G1 phases) was determined under various conditions and plotted in [Figure 4](#). The figure shows that the distribution of control cells grown in complete medium in G1, S, G2/M, and sub-G1 phases was  $\sim$ 59,  $\sim$ 16,  $\sim$ 23, and  $\sim$ 2%, respectively. In the case of cells cultured under hypoxic conditions, we observed a significant increase in cell numbers in the G1 phase of the cell cycle across all time points. These results indicate the arrest of cell cycle at the G1/S interphase.

**Ligand Binding to the Serotonin<sub>1A</sub> Receptor under Hypoxic Conditions.** Ligand binding to GPCRs is the first step toward initiation of signaling in response to an extracellular stimulus. In order to monitor the changes in ligand binding to the serotonin<sub>1A</sub> receptor upon hypoxia, we carried out whole cell ligand binding of the serotonin<sub>1A</sub> receptor. Importantly, we previously showed that the serotonin<sub>1A</sub> receptor expressed in CHO-K1 cells with the C-

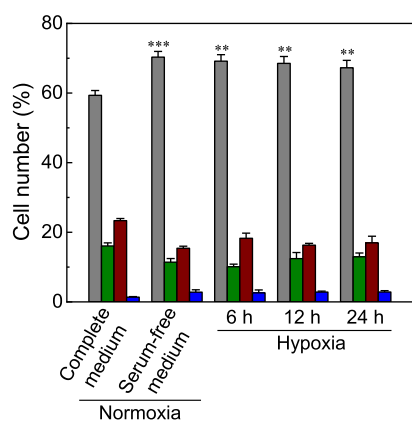


**Figure 4.** Effect of hypoxia on cell cycle. Cell cycle arrest was monitored in cells cultured under hypoxic conditions for 6, 12, and 24 h. Cell numbers in G1, S, G2/M, and sub-G1 phases are represented by gray, green, maroon, and blue bars, respectively. Data represent means  $\pm$  SE from at least three independent experiments (\*\* and \*\*\* correspond to significant ( $p < 0.01$  and  $p < 0.001$ ) difference in the number of cells at G1 phase under hypoxic conditions and cells grown in serum-free media under normoxic conditions relative to cells grown in complete medium, respectively). See [Methods](#) for more details.

terminal EYFP tag (CHO-5-HT<sub>1A</sub>R-EYFP) retains all the characteristics of the native receptor in terms of ligand binding, G-protein coupling, and signaling.<sup>58</sup> [Figure 5](#) shows a specific radiolabeled agonist ([<sup>3</sup>H]8-OH-DPAT) binding to the serotonin<sub>1A</sub> receptor under normoxic and hypoxic conditions. The figure shows a progressive reduction in the specific agonist binding to the serotonin<sub>1A</sub> receptor in cells upon exposure to hypoxia. We observed a significant reduction of ~43 and ~58%

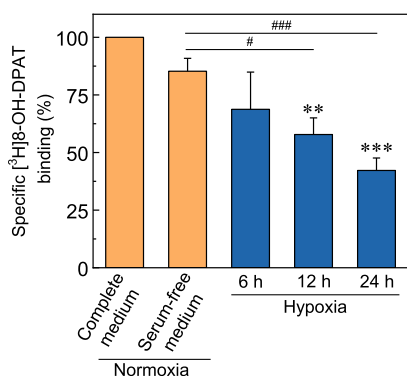


**Figure 5.** Effect of hypoxia on agonist binding to the serotonin<sub>1A</sub> receptor. Specific binding of the radiolabeled agonist [<sup>3</sup>H]8-OH-DPAT to serotonin<sub>1A</sub> receptors in intact CHO-5-HT<sub>1A</sub>R-EYFP cells exposed to hypoxic conditions for 6, 12, and 24 h (blue bars). The corresponding data for cells maintained under normoxic conditions are also shown (orange bars). Values are expressed as percentages of specific radioligand binding normalized to control cells grown in complete medium under normoxic conditions. Data represent means  $\pm$  SE from at least three independent experiments (\*\* and \*\*\* correspond to significant ( $p < 0.01$  and  $p < 0.0001$ ) difference in specific [<sup>3</sup>H]8-OH-DPAT binding in cells cultured under hypoxic conditions for 12 and 24 h, respectively, relative to cells grown in complete medium under normoxic conditions; # and ### correspond to significant ( $p < 0.05$  and  $p < 0.001$ ) difference in specific [<sup>3</sup>H]8-OH-DPAT binding in cells cultured under hypoxic conditions for 12 and 24 h, respectively, relative to cells grown in serum-free medium under normoxic conditions). See [Methods](#) for more details.

in specific agonist binding in cells exposed to hypoxic conditions for 12 and 24 h, respectively, relative to the cells cultured in complete medium under normoxic conditions.

**Expression of the Serotonin<sub>1A</sub> Receptor under Hypoxic Conditions.** The observed decrease in the ligand binding activity of the serotonin<sub>1A</sub> receptor could be due to the change in the receptor expression under hypoxic conditions. To rule out any change in the receptor expression level under hypoxic conditions, we analyzed the receptor expression level using a flow cytometry-based assay. Flow cytometry is a robust, population-based method, which allows to quantitatively monitor the presence of fluorescently tagged molecules in cells. In our assay, we utilized the fluorescence signal from the EYFP-tagged serotonin<sub>1A</sub> receptor as a measure of receptor level under various conditions. [Figure 6a](#) shows the representative flow cytometric histograms depicting the distribution of EYFP fluorescence in cells grown under normoxic and hypoxic conditions. To quantitate the number of cells with high EYFP fluorescence, we used an untagged version (without EYFP) of the serotonin<sub>1A</sub> receptor to gate EYFP-negative cells (first panel in [Figure 6a](#)). A shift in the fluorescence histogram toward lower values on the fluorescence axis would indicate the reduction in the population of receptors in cells. The reduction in the mean fluorescence intensity due to such shift in the flow cytometric histogram is indicative of reduction in the receptor population under hypoxia. [Figure 6b](#) shows that there was no significant change in the EYFP-positive population of the serotonin<sub>1A</sub> receptor upon hypoxia. In addition, [Figure 6c](#) shows that there was no significant change in the mean fluorescence intensity of the flow cytometric histograms across all conditions, indicating that the reduction in ligand binding under hypoxic conditions was not due to the altered receptor levels. These results suggest that the reduced ligand binding to the serotonin<sub>1A</sub> receptor could be due to the reduction in agonist binding affinity to the receptor.

**Serotonin<sub>1A</sub> Receptor Downstream Signaling is Compromised under Hypoxia.** Agonist binding to the human serotonin<sub>1A</sub> receptor activates the Gi/Go class of G-proteins in CHO cells,<sup>66</sup> resulting in the inhibition of adenylyl cyclase activity which results in the decrease in cellular cAMP levels.<sup>67</sup> To assess the effect of hypoxia on the signaling efficacy of the serotonin<sub>1A</sub> receptor, we monitored the serotonin (agonist)-stimulated reduction of cAMP levels by the serotonin<sub>1A</sub> receptor in these conditions. As the basal levels of cAMP are low (therefore difficult to measure), the cellular level of cAMP first needs to be increased using agents such as forskolin to assess the Gi-mediated reduction in cAMP levels. We utilized a FRET-based assay<sup>68–70</sup> to quantify serotonin-induced reduction in forskolin-stimulated cAMP levels. The relative reduction in cAMP levels mediated by the serotonin<sub>1A</sub> receptor upon treatment with serotonin, normalized to that found upon forskolin stimulation alone, is shown in [Figure 7](#). The figure clearly shows that culturing cells under hypoxic conditions leads to a reduction in serotonin-stimulated cAMP levels relative to control cells. There was a significant reduction in cellular signaling mediated by the serotonin<sub>1A</sub> receptor in the cases of 12 and 24 h hypoxic treatment. As a control, cells grown in serum-free medium for 24 h under normoxic conditions did not exhibit any reduction in cellular signaling. The reduction in cAMP signaling under hypoxic conditions, therefore, could be attributed to low oxygen levels. Taken

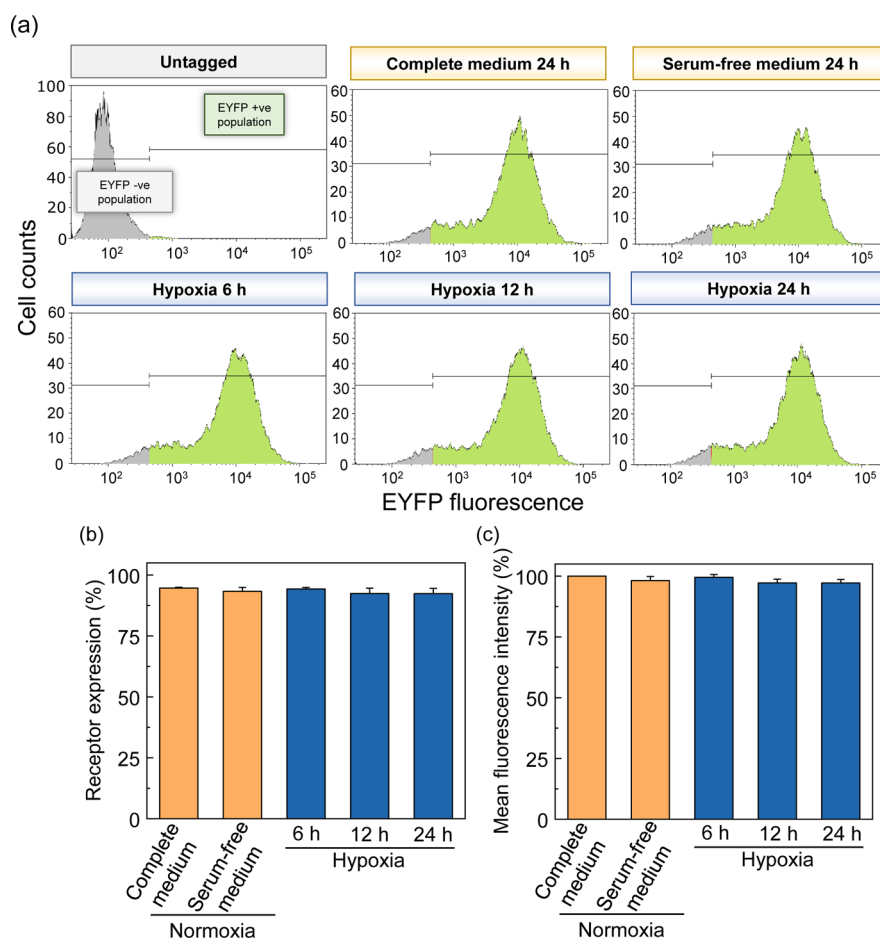


**Figure 6.** Effect of hypoxia on the expression of the serotonin<sub>1A</sub> receptor in CHO-5-HT<sub>1A</sub>-R-EYFP cells. (a) Receptor expression was analyzed using a flow cytometry-based assay using the EYFP-tagged serotonin<sub>1A</sub> receptor. Representative flow cytometric histograms showing the population of the serotonin<sub>1A</sub> receptor tagged to EYFP at its C-terminal under hypoxic conditions. CHO-K1 cells expressing an untagged (without EYFP) version of the serotonin<sub>1A</sub> receptor were used to gate EYFP-negative (gray regions denoted as EYFP-negative) and EYFP (green regions denoted as EYFP-positive) population of cells. Quantification of the serotonin<sub>1A</sub> receptor expression as measured by (b) percentage of EYFP-positive cells from flow cytometric histograms and (c) mean fluorescence intensity. Values are expressed as percentage of EYFP-positive cells in each condition. Data represent means  $\pm$  SE from at least three independent experiments (no significant differences observed in the receptor expression in cells cultured under hypoxic conditions relative to control cells in both cases). See [Methods](#) for more details.

together, these results show that the signaling efficiency of the serotonin<sub>1A</sub> receptor is compromised in a hypoxic condition.

## DISCUSSION

Hypoxia is a physiological stress condition caused due to the lack of oxygen in cells, which leads to organ dysfunction and tissue necrosis.<sup>8</sup> Cerebral hypoxia could cause widespread brain damage and atrophy, leading to amnesia, depression, and anxiety.<sup>56,71</sup> As cognitive disability, depression, and anxiety are commonly associated with the malfunction of the serotonin<sub>1A</sub> receptor,<sup>72,73</sup> we explored the association between hypoxia and the function of the serotonin<sub>1A</sub> receptor. For this, we generated a cellular hypoxia model mimicking the effect of moderate hypoxia, characterized by the accumulation of lanosterol in cells<sup>22</sup> and the arrest of cell cycle at the G1 phase.<sup>18</sup> Interestingly, membrane cholesterol has been reported to regulate the cell cycle progression.<sup>30,31</sup> We previously showed that the presence of immediate biosynthetic precursors of cholesterol (such as 7-dehydrocholesterol and desmosterol) could induce cell cycle arrest.<sup>30</sup> We observed that a prolonged exposure (12 and 24 h) of cells to hypoxic conditions led to reduction in ligand binding and cAMP signaling by the

serotonin<sub>1A</sub> receptor. Interestingly, the progressive accumulation of lanosterol in cells exposed to prolonged hypoxia (12 and 24 h) correlated with the dysfunction of the serotonin<sub>1A</sub> receptor.

The serotonin<sub>1A</sub> receptor is primarily expressed in the central nervous system, as evident from the neurological functions associated with the receptor. Autoradiography using specific radiolabeled agonists and antagonists of the receptor showed that the serotonin<sub>1A</sub> receptor is highly expressed in the limbic forebrain regions such as the hippocampus, raphe nuclei, amygdala, hypothalamus, and cortex, whereas the lowest density is found in the extrapyramidal areas such as the basal ganglia, substantia nigra, and in the adult cerebellum.<sup>34,74</sup> Notably, under normoxic conditions, the partial pressure of oxygen ( $p_{O_2}$ ) in brain is  $\sim$ 34 mmHg (4.6%  $p_{O_2}$ ).<sup>75-79</sup> A drop in oxygen levels below this value would create a hypoxic condition in the brain.<sup>8</sup>

Defects in cholesterol biosynthesis have been reported to cause impaired synaptic transduction and neurodegenerative disorders.<sup>80</sup> Cholesterol is synthesised *de novo* in the CNS<sup>81</sup> and accounts for  $\sim$ 25% of the total cholesterol content in the body.<sup>82-84</sup> Accumulation of cholesterol biosynthetic precursors

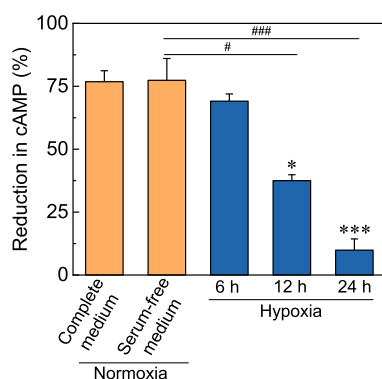


**Figure 7.** Effect of hypoxia on cAMP signaling mediated by the serotonin<sub>1A</sub> receptor. The efficiency of the serotonin<sub>1A</sub> receptor to inhibit forskolin-stimulated increase in cAMP levels by activation with 10  $\mu$ M serotonin in CHO-5-HT<sub>1A</sub>R cells exposed to hypoxic conditions. Data are normalized to cAMP levels in the presence of 50  $\mu$ M IBMX + 10  $\mu$ M forskolin (forskolin-stimulated) for each condition. Data represent means  $\pm$  SE of at least four independent experiments (\* and \*\*\* correspond to significant ( $p < 0.05$  and  $p < 0.0001$ ) difference in reduction in cAMP content in cells cultured under hypoxic conditions for 12 and 24 h, respectively, relative to cells grown in complete medium under normoxic conditions; # and ### correspond to significant ( $p < 0.05$  and  $p < 0.001$ ) difference in reduction in cAMP content in cells cultured under hypoxic conditions for 12 and 24 h, respectively, relative to cells grown in serum-free medium under normoxic conditions). See Methods for more details.

sors in the brain, as a consequence of the inhibition of cholesterol pathway, has been associated with various neurological diseases.<sup>80,85</sup> The serotonin<sub>1A</sub> receptor, a critical neurotransmitter receptor in the GPCR family, displays a stringent requirement for cholesterol, both in terms of its structure<sup>86,87</sup> and optimal level,<sup>88</sup> for its organization, dynamics, and function. Cholesterol sensitivity to GPCR function can be attributed to the direct interaction of membrane cholesterol with GPCRs, or by cholesterol-induced changes in the global lipid bilayer properties, or a combination of both mechanisms.<sup>89</sup> In this context, cholesterol interaction motifs represent putative sites on receptors that could be involved in facilitating specific interactions with cholesterol.<sup>90</sup> Notably, we recently showed that a key lysine residue (K101), that forms a part of the cholesterol recognition/interaction amino acid consensus (CRAC) motif in the transmembrane helix 2 of the serotonin<sub>1A</sub> receptor, is crucial in sensing altered membrane cholesterol levels.<sup>70</sup> In general, changes in membrane properties due to sterol modulation have earlier been shown to lead to the modulation of membrane phospholipids.<sup>91</sup> On a cautionary note, we would therefore like to mention that changes in lipidome (other than sterols) upon hypoxia have been previously reported.<sup>92–95</sup> In this context, we observed the appearance of a few nonidentified bands on the thin-layer chromatogram under hypoxic conditions, apart from the marked accumulation of lanosterol (Figure 3a). The contribution of nonsterol lipids in the impaired function of the serotonin<sub>1A</sub> receptor, therefore, may not be ruled out.

Taken together, our results highlight the impaired function of the serotonin<sub>1A</sub> receptor under hypoxic conditions, which could be relevant in understanding cerebral hypoxia that has been a major point of concern for mountaineers and soldiers stationed at high altitudes.<sup>96</sup> We believe that our results constitute one of the first reports linking altered serotonin<sub>1A</sub>

receptor function with hypoxia and could provide opportunities for novel therapeutics in hypoxia-related disorders. From a broader perspective, our work represents an important step in understanding the link between oxygen, sterol biosynthesis, and function of neuronal receptors, thereby contributing to our overall understanding of the molecular basis underlying neurological conditions often associated with hypoxia-induced brain dysfunction.

## METHODS

**Materials.** Bovine serum albumin, cholesterol, trypsin, EDTA, forskolin, gentamycin sulfate, 3-isobutyl-1-methylxanthine (IBMX), genistein (G418), lanosterol, sodium bicarbonate, penicillin, streptomycin, phenylmethylsulfonyl fluoride (PMSF), polyethylenimine, serotonin, Tris, PI, RNase A, and staurosporine were purchased from Sigma Chemical Co. (St. Louis, MO). Bicinchoninic acid (BCA) reagent for protein estimation was obtained from Pierce (Rockford, IL). [<sup>3</sup>H]8-Hydroxy-2-(di-*N*-propylamino)tetralin ([<sup>3</sup>H]8-OH-DPAT, specific activity: 141.1 Ci/mmol) was obtained from MP Biomedicals (Santa Ana, CA). DMEM/F-12 [Dulbecco's modified Eagle's medium/nutrient mixture F-12 (Ham) (1:1)] and fetal calf serum were obtained from Gibco/Life Technologies (Grand Island, NY). Amplex Red cholesterol assay kit was purchased from Molecular Probes/Invitrogen (Eugene, OR). GF/B glass microfiber filters were obtained from Whatman International (Kent, UK). Homogeneous time-resolved fluorescence (HTRF) cAMP-Gi assay kit was purchased from CisBio Bioassays (Codolet, France). Precoated silica gel 60 thin-layer chromatography plates were obtained from Merck (Darmstadt, Germany). ApoAlert Annexin V apoptosis kit was purchased from Clontech Laboratories (Mountain View, CA). All chemicals used were of the highest available purity. Water was purified through a Millipore (Bedford, MA) Milli-Q system and used throughout.

**Cell Culture under Normoxic and Hypoxic Conditions.** CHO-K1 cells stably expressing human serotonin<sub>1A</sub> receptors tagged to EYFP at its C-terminus (CHO-5-HT<sub>1A</sub>R-EYFP) were maintained in DMEM/F-12 (1:1) medium, supplemented with 2.4 g/L of sodium bicarbonate, 10% (v/v) fetal calf serum, 60  $\mu$ g/mL penicillin, 50  $\mu$ g/mL streptomycin, 50  $\mu$ g/mL gentamycin sulfate (complete medium), and 0.3 mg/mL G418 in a humidified atmosphere with 5% CO<sub>2</sub> at 37 °C for 72 h.<sup>58</sup> CHO-5-HT<sub>1A</sub>R cells (receptors without EYFP tag) were maintained in complete medium with 0.2 mg/mL G418<sup>57</sup> under the same conditions for 72 h (or 84 h or 90 h, depending on the time in the hypoxic chamber so that the total time remains 96 h in all cases). Cells were cultured under hypoxic conditions at 1% O<sub>2</sub> and 5% CO<sub>2</sub> at 37 °C in a humidified HERA CELL 240i CO<sub>2</sub> incubator (where O<sub>2</sub> concentration could be regulated using excess nitrogen) in serum-free medium for 6, 12, or 24 h. Two control groups of cells were grown in complete and serum-free media under normoxic conditions (21% O<sub>2</sub> and 5% CO<sub>2</sub> at 37 °C) for 24 h. We plated  $\sim$ 10<sup>5</sup> cells in 35 mm culture dish (for cAMP assay),  $\sim$ 5  $\times$  10<sup>5</sup> cells in 100 mm culture dish (for quantifying receptor expression, apoptosis assay, radioligand binding assay, and cell cycle analysis), and  $\sim$ 15  $\times$  10<sup>5</sup> cells in 150 mm culture dish (for thin-layer chromatography and cholesterol estimation).

**Cell Membrane Preparation.** Subsequent to treatments, cells were washed with phosphate-buffered saline (PBS) and harvested by treatment with ice-cold hypotonic buffer containing 10 mM Tris, 5 mM EDTA, and 0.1 mM PMSF (pH 7.4).<sup>57</sup> Cells were then homogenized for 10 s using a Polytron homogenizer at a maximum speed. The homogenized cells were centrifuged at 500g for 10 min at 4 °C. The resulting supernatant was centrifuged at 40,000g for 30 min at 4 °C, and pellets were suspended in 50 mM Tris buffer, pH 7.4. The total protein concentration in isolated membranes was determined using BCA assay.<sup>97</sup>

**Detection of Lanosterol and Cholesterol by Thin-Layer Chromatography.** Total lipids were extracted from isolated cell membranes according to the Bligh and Dyer method.<sup>98</sup> The extracted lipids were dried using a stream of nitrogen at  $\sim$ 45 °C and dissolved using a mixture of chloroform/methanol (1:1, v/v). Sterols were

visualized by thin-layer chromatography using precoated silica gel plates. Sterols were resolved in a dual solvent system, using ethyl acetate/benzene (1:5, v/v) as the first solvent system and heptane/benzene (97:3, v/v) as the second solvent system.<sup>99</sup> The first solvent was allowed to run for about three-fourth length of the plate and dried under hot air before running the entire length of the plate in the second solvent system. The separated lipids were visualized by charring with a solution containing cupric sulfate (10%, w/v) and orthophosphoric acid (8%, v/v) at 150 °C. Lanosterol and cholesterol bands were identified using respective standards. The TLC plates were scanned, and sterol band intensities were estimated using densitometric analysis of the chromatogram using Adobe Photoshop CS3 (Adobe Systems, San Jose, California) software.

**Estimation of Cholesterol Content.** The cholesterol content in cell membranes was estimated using the Amplex Red cholesterol assay kit<sup>60</sup> and normalized to the total cellular protein estimated using the BCA assay.<sup>97</sup>

**Detection of Apoptosis.** The percentage of apoptotic cells was assessed by flow cytometry using an Annexin V-FITC/PI apoptosis detection kit as per manufacturer's protocol. CHO-5-HT<sub>1A</sub>R cells were collected after treatment with 0.1% (w/v) trypsin-EDTA and washed with complete DMEM/F-12 medium. The cells were further washed with 1× binding buffer and incubated with 5 μL of Annexin V-FITC (stock concentration, 20 μg/mL) and 10 μL of PI (stock concentration, 50 μg/mL) at a density of ~5 × 10<sup>6</sup> cells/mL in 1× binding buffer for 15 min at room temperature (~23 °C) in the dark. The samples were analyzed using a Gallios flow cytometer (Beckman Coulter, Brea, CA). FITC and PI were excited at 488 nm, and the emission was collected using 525/40 and 620/30 nm bandpass filters, respectively. As a positive control, cells were treated with 5 μM staurosporine for 24 h in a humidified atmosphere with 5% CO<sub>2</sub> at 37 °C. The acquired data were analyzed using Kaluza analysis software (version 1.5a, Beckman Coulter, Brea, CA).

**Flow Cytometric Analysis of Cell Cycle.** CHO-5-HT<sub>1A</sub>R cells were harvested using 0.1% (w/v) trypsin-EDTA, centrifuged for 5 min at 500g, and fixed using ice-cold 70% (v/v) ethanol for 10 min. Subsequently, cells were centrifuged, and DNA was labeled in PBS containing 2% (v/v) FCS with 50 μg/mL PI and 200 μg/mL RNase A. Cells were incubated for 15 min in the staining solution on ice, centrifuged, and resuspended in PBS containing 2% (v/v) FCS. The distribution of cells in the different phases of cell cycle was monitored using a Gallios flow cytometer (Beckman Coulter, Brea, CA), and the acquired data were analyzed using Kaluza analysis software (version 1.5a, Beckman Coulter, Brea, CA). The excitation was set at 488 nm, and emission was collected using a 620/30 nm bandpass filter, while 10,000 cells were analyzed in each condition. To distinguish single cells from multiplets of cells, we used a "pulse-processing" protocol, where fluorescence from multiplets of cells was excluded using a fluorescence pulse width and fluorescence pulse area display.<sup>30</sup>

**Radioligand Binding Assay in Live Cells.** CHO-5-HT<sub>1A</sub>R-EYFP cells were harvested using PBS containing 0.25 mM EDTA. Cells were spun at 500g for 5 min and resuspended in serum-free DMEM/F-12 medium for counting using a hemocytometer. Cells (~10<sup>6</sup>) in serum-free medium were incubated at 25 °C for 15 min in the presence of 1 nM [<sup>3</sup>H]8-OH-DPAT. Nonspecific binding was obtained by performing the assay in the presence of 10 μM unlabeled serotonin. Ligand binding was terminated by rapid filtration under vacuum through a Millipore multiport filtration apparatus using Whatman GF/B glass microfiber filters of 1 μM pore size that were presoaked in 0.3% (w/v) polyethylenimine for 3 h. This was followed by washing the filters three times with 5 mL of ice-cold water (~4 °C). After subsequent drying of the filters, the remaining radioactivity was measured using ~5 mL scintillation fluid in a Packard Tri-Carb 2900 liquid scintillation counter (PerkinElmer, Waltham, MA).

**Flow Cytometric Analysis of Receptor Expression Level.** CHO-5-HT<sub>1A</sub>R-EYFP cells were collected in PBS containing 0.25 mM EDTA, spun at 500g for 5 min, and resuspended in PBS containing 2% (v/v) FCS. The receptor population from 10,000 cells in each condition was quantified using a Gallios flow cytometer (Beckman Coulter, Brea, CA), and data were acquired and analyzed

using Kaluza analysis software (version 1.5a, Beckman Coulter, Brea, CA). Excitation was set at 488 nm, and emission was collected using a 525/40 nm bandpass filter. CHO-5-HT<sub>1A</sub>R (serotonin<sub>1A</sub> receptors without EYFP tag) cells were used to gate EYFP-negative population.

**Cellular Signaling Assay.** CHO-5-HT<sub>1A</sub>R cells were treated with 50 μM IBMX (basal), 50 μM IBMX + 10 μM forskolin (forskolin-stimulated), or 50 μM IBMX + 10 μM forskolin + 10 μM serotonin (agonist treatment) and incubated for 30 min at 37 °C. The phosphodiesterase inhibitor IBMX was present during all treatments to prevent the breakdown of cAMP. Incubation was performed under hypoxic conditions for cells previously grown under hypoxia, whereas control cells were incubated under normoxic conditions. After discarding the media, cells were washed once with PBS, lifted using a cell scraper, counted using a hemocytometer, and added at 6000 cells/well to a low-volume HTRF 96-well plate (CisBio Bioassays). The ability of the serotonin<sub>1A</sub> receptor to inhibit the forskolin-stimulated increase in cAMP levels was assessed using the fluorescence resonance energy transfer (FRET)-based HTRF cAMP-Gi assay kit (CisBio Bioassays). Fluorescence was measured at 620 nm (cAMP-cryptate donor emission) and 655 nm (anti-cAMP-d2 acceptor emission) upon excitation of the donor at 320 nm using the EnSpire Multimode Plate Reader (PerkinElmer, Waltham, MA). cAMP levels were calculated as a ratio of the acceptor/donor emission. Values for serotonin-induced cAMP reduction were normalized to cAMP levels in the presence 50 μM IBMX + 10 μM forskolin-treated cells.<sup>70,100</sup>

## STATISTICAL ANALYSIS

Significance levels were analyzed using Student's two-tailed unpaired *t* test using GraphPad Prism software, version 4.0 (San Diego, CA). Plots were generated using OriginPro software, version 8.0 (OriginLab, Northampton, MA).

## ASSOCIATED CONTENT

### Supporting Information

The Supporting Information is available free of charge at <https://pubs.acs.org/doi/10.1021/acscchemneuro.2c00181>.

Treatment conditions for generating cellular hypoxia model and effect of hypoxia on apoptosis (PDF)

## AUTHOR INFORMATION

### Corresponding Author

Amitabha Chattopadhyay – CSIR-Centre for Cellular and Molecular Biology, Hyderabad 500 007, India; [orcid.org/0000-0002-2618-2565](https://orcid.org/0000-0002-2618-2565); Phone: +91-40-2719-2578; Email: [amit@ccmb.res.in](mailto:amit@ccmb.res.in)

### Authors

Aritri Dutta – CSIR-Centre for Cellular and Molecular Biology, Hyderabad 500 007, India

Parijat Sarkar – CSIR-Centre for Cellular and Molecular Biology, Hyderabad 500 007, India

Sandeep Shrivastava – CSIR-Centre for Cellular and Molecular Biology, Hyderabad 500 007, India

Complete contact information is available at: <https://pubs.acs.org/10.1021/acscchemneuro.2c00181>

### Author Contributions

A.D. and P.S. have equal contribution. A.D. and P.S. performed experiments and analyzed the data; A.D., S.S., and A.C. designed the project framework; A.D., P.S., and A.C. designed the experiments; A.D., P.S., and A.C. wrote the manuscript. A.C. conceptualized the project, edited the manuscript, organized access to research facilities and funding, and provided overall supervision and mentoring.

## Notes

The authors declare no competing financial interest.

## ACKNOWLEDGMENTS

A.C. gratefully acknowledges support from CSIR Bhatnagar Fellowship and SERB Distinguished Fellowship. A.D. thanks the Council of Scientific and Industrial Research for the award of Research Associateship. P.S. was supported as a Senior Project Associate by a CSIR FBR Grant to A.C. (MLP 0146). The authors thank Gunda Srinivas for help with acquiring flow cytometric data and Suman Bandari for his help with preliminary experiments. They gratefully acknowledge the members of the Chattopadhyay laboratory and G. Aditya Kumar and Sreetama Pal for their comments and suggestions.

## ABBREVIATIONS

FITC, fluorescein isothiocyanate; PI, propidium iodide; ER, endoplasmic reticulum; BCA, bicinchoninic acid; EDTA, ethylenediaminetetraacetic acid; CHO, Chinese hamster ovary; PBS, phosphate-buffered saline; cAMP, adenosine 3',5'-cyclic monophosphate; FRET, fluorescence resonance energy transfer; IBMX, 3-isobutyl-1-methylxanthine; 8-OH-DPAT, 8-hydroxy-2-(di-N-propylamino)tetralin

## REFERENCES

- (1) Des Marais, D. J. When did photosynthesis emerge on earth? *Science* **2000**, *289*, 1703.
- (2) Hedges, S. B.; Blair, J. E.; Venturi, M. L.; Shoe, J. L. A molecular timescale of eukaryote evolution and the rise of complex multicellular life. *BMC Evol. Biol.* **2004**, *4*, 2.
- (3) Raymond, J.; Blankenship, R. E. Biosynthetic pathways, gene replacement and the antiquity of life. *Geobiol* **2004**, *2*, 199–203.
- (4) Galea, A. M.; Brown, A. J. Special relationship between sterols and oxygen: Were sterols an adaptation to aerobic life? *Free Radical Biol. Med.* **2009**, *47*, 880–889.
- (5) Brown, A. J.; Galea, A. M. Cholesterol as an evolutionary response to living with oxygen. *Evol* **2010**, *64*, 2179–2183.
- (6) Gilany, K.; Vafakhah, M. Hypoxia: A review. *J. Paramed. Sci.* **2010**, *1*, 43–60.
- (7) Michiels, C. Physiological and pathological responses to hypoxia. *Am. J. Pathol.* **2004**, *164*, 1875–1882.
- (8) Carreau, A.; Hafny-Rahbi, B. E.; Matejuk, A.; Grillon, C.; Kieda, C. Why is the partial oxygen pressure of human tissues a crucial parameter? Small molecules and hypoxia. *J. Cell. Mol. Med.* **2011**, *15*, 1239–1253.
- (9) Baik, A. H.; Jain, I. H. Tuning the oxygen dial: Balancing the highs and lows. *Trends Cell Biol.* **2020**, *30*, 516–536.
- (10) Li, J.; Qi, Y.; Liu, H.; Cui, Y.; Zhang, L.; Gong, H.; Li, Y.; Li, L.; Zhang, Y. Acute high-altitude hypoxic brain injury: Identification of ten differential proteins. *Neural Regen. Res.* **2013**, *8*, 2932–2941.
- (11) Couzin-Frankel, J. The mystery of the pandemic's "happy hypoxia". *Science* **2020**, *368*, 455–456.
- (12) Rapalino, O.; Weerasekera, A.; Moum, S. J.; Eikermann-Haerter, K.; Edlow, B. L.; Fischer, D.; Torrado-Carvajal, A.; Loggia, M. L.; Mukerji, S. S.; Schaefer, P. W.; Gonzalez, R. G.; Lev, M. H.; Ratai, E.-M. Brain MR spectroscopic findings in 3 consecutive patients with COVID-19: Preliminary observations. *Am. J. Neuroradiol.* **2021**, *42*, 37–41.
- (13) Raichle, M. E.; Gusnard, D. A. Appraising the brain's energy budget. *Proc. Natl. Acad. Sci. U.S.A.* **2002**, *99*, 10237–10239.
- (14) Busl, K. M.; Greer, D. M. Hypoxic-ischemic brain injury: Pathophysiology, neuropathology and mechanisms. *NeuroRehabilitation* **2010**, *26*, 5–13.
- (15) Semenza, G. L. Oxygen sensing, hypoxia-inducible factors, and disease pathophysiology. *Annu. Rev. Pathol.: Mech. Dis.* **2014**, *9*, 47–71.

- (16) Gardner, L. B.; Li, Q.; Park, M. S.; Flanagan, W. M.; Semenza, G. L.; Dang, C. V. Hypoxia inhibits G1/S transition through regulation of p27 expression. *J. Biol. Chem.* **2001**, *276*, 7919–7926.
- (17) Lee, P.; Chandel, N. S.; Simon, M. C. Cellular adaptation to hypoxia through hypoxia inducible factors and beyond. *Nat. Rev. Mol. Cell Biol.* **2020**, *21*, 268–283.
- (18) Goda, N.; Ryan, H. E.; Khadivi, B.; McNulty, W.; Rickert, R. C.; Johnson, R. S. Hypoxia-inducible factor 1 $\alpha$  is essential for cell cycle arrest during hypoxia. *Mol. Cell. Biol.* **2003**, *23*, 359–369.
- (19) Mylonis, I.; Simos, G.; Paraskeva, E. Hypoxia-inducible factors and the regulation of lipid metabolism. *Cells* **2019**, *8*, 214.
- (20) Summons, R. E.; Bradley, A. S.; Jahnke, L. L.; Waldbauer, J. R. Steroids, triterpenoids and molecular oxygen. *Philos. Trans. R. Soc. London, Ser. B* **2006**, *361*, 951–968.
- (21) Bloch, K. E. Evolutionary Perfection of a Small Molecule. In *Blondes in Venetian Paintings, the Nine-Banded Armadillo, and Other Essays in Biochemistry*; Yale University Press: New Haven, 1994; Chapter 2, pp 14–36.
- (22) Nguyen, A. D.; McDonald, J. G.; Bruick, R. K.; DeBose-Boyd, R. A. Hypoxia stimulates degradation of 3-hydroxy-3-methylglutaryl-coenzyme A reductase through accumulation of lanosterol and hypoxia-inducible factor-mediated induction of insigs. *J. Biol. Chem.* **2007**, *282*, 27436–27446.
- (23) DeBose-Boyd, R. A. Feedback regulation of cholesterol synthesis: Sterol-accelerated ubiquitination and degradation of HMG CoA reductase. *Cell Res.* **2008**, *18*, 609–621.
- (24) Maxfield, F. R.; van Meer, G. Cholesterol, the central lipid of mammalian cells. *Curr. Opin. Cell Biol.* **2010**, *22*, 422–429.
- (25) Kumar, G. A.; Chattopadhyay, A. Cholesterol: An evergreen molecule in biology. *Biomed. Spectrosc. Imaging* **2016**, *5*, S55–S66.
- (26) Stevenson, J.; Brown, A. J. How essential is cholesterol? *Biochem. J.* **2009**, *420*, e1–e4.
- (27) Mukherjee, S.; Maxfield, F. R. Membrane domains. *Annu. Rev. Cell Dev. Biol.* **2004**, *20*, 839–866.
- (28) Bernsdorff, C.; Winter, R. Differential properties of the sterols cholesterol, ergosterol,  $\beta$ -sitosterol, trans-7-dehydrocholesterol, stigmasterol and lanosterol on DPPC bilayer order. *J. Phys. Chem. B* **2003**, *107*, 10658–10664.
- (29) Russell, D. W. Cholesterol biosynthesis and metabolism. *Cardiovasc. Drugs Ther.* **1992**, *6*, 103–110.
- (30) Singh, P.; Saxena, R.; Srinivas, G.; Pande, G.; Chattopadhyay, A. Cholesterol biosynthesis and homeostasis in regulation of cell cycle. *PLoS One* **2013**, *8*, No. e58833.
- (31) Sarkar, P.; Rao, B. D.; Chattopadhyay, A. Cell-cycle dependent modulation of membrane dipole potential and neurotransmitter receptor activity: Role of membrane cholesterol. *ACS Chem. Neurosci.* **2020**, *11*, 2890–2899.
- (32) Chattopadhyay, A. GPCRs: Lipid-dependent membrane receptors that act as drug targets. *Adv. Biol.* **2014**, *2014*, 143023.
- (33) Insel, P. A.; Sriram, K.; Gorr, M. W.; Wiley, S. Z.; Michkov, A.; Salmerón, C.; Chinn, A. M. GPCRomics: An approach to discover GPCR drug targets. *Trends Pharmacol. Sci.* **2019**, *40*, 378–387.
- (34) Pucadyil, T. J.; Kalipatnapu, S.; Chattopadhyay, A. The serotonin<sub>1A</sub> receptor: A representative member of the serotonin receptor family. *Cell. Mol. Neurobiol.* **2005**, *25*, 553–580.
- (35) Müller, C. P.; Carey, R. J.; Huston, J. P.; De Souza Silva, M. A. Serotonin and psychostimulant addiction: Focus on 5-HT<sub>1A</sub>-receptors. *Prog. Neurobiol.* **2007**, *81*, 133–178.
- (36) Sarkar, P.; Kumar, G. A.; Pal, S.; Chattopadhyay, A. Biophysics of Serotonin and the Serotonin<sub>1A</sub> Receptor: Fluorescence and Dynamics. In *Serotonin: The Mediator That Spans Evolution*; Pilowsky, P., Ed.; Elsevier: Amsterdam, 2018; pp 3–22.
- (37) Sarkar, P.; Mozumder, S.; Bej, A.; Mukherjee, S.; Sengupta, J.; Chattopadhyay, A. Structure, dynamics and lipid interactions of serotonin receptors: Excitements and challenges. *Biophys. Rev.* **2021**, *13*, 101–122.
- (38) Carhart-Harris, R.; Nutt, D. Serotonin and brain function: Tale of two receptors. *J. Psychopharmacol.* **2017**, *31*, 1091–1120.

- (39) Lacivita, E.; Leopoldo, M.; Berardi, F.; Perrone, R. 5-HT<sub>1A</sub> receptor, an old target for new therapeutic agents. *Curr. Top. Med. Chem.* **2008**, *8*, 1024–1034.
- (40) Celada, P.; Bortolozzi, A.; Artigas, F. Serotonin 5-HT<sub>1A</sub> receptors as targets for agents to treat psychiatric disorders: Rationale and current status of research. *CNS Drugs* **2013**, *27*, 703–716.
- (41) Fiorino, F.; Severino, B.; Magli, E.; Ciano, A.; Caliendo, G.; Santagada, V.; Frecentese, F.; Perissutti, E. 5-HT<sub>1A</sub> receptor: An old target as a new attractive tool in drug discovery from central nervous system to cancer. *J. Med. Chem.* **2014**, *57*, 4407–4426.
- (42) Fu, X. W.; Nurse, C. A.; Wong, V.; Cutz, E. Hypoxia-induced secretion of serotonin from intact pulmonary neuroepithelial bodies in neonatal rabbit. *J. Physiol.* **2002**, *539*, 503–510.
- (43) Esteve, J. M.; Launay, J.-M.; Kellermann, O.; Maroteaux, L. Functions of serotonin in hypoxic pulmonary vascular remodeling. *Cell Biochem. Biophys.* **2007**, *47*, 33–43.
- (44) Kumar, G. K. Hypoxia. 3. Hypoxia and neurotransmitter synthesis. *Am. J. Physiol.: Cell Physiol.* **2011**, *300*, C743–C751.
- (45) Fanburg, B. L.; Lee, S.-L. A role for the serotonin transporter in hypoxia-induced pulmonary hypertension. *J. Clin. Invest.* **2000**, *105*, 1521–1523.
- (46) Eddahibi, S.; Fabre, V.; Boni, C.; Martres, M. P.; Raffestin, B.; Hamon, M.; Adnot, S. Induction of serotonin transporter by hypoxia in pulmonary vascular smooth muscle cells. Relationship with the mitogenic action of serotonin. *Circ. Res.* **1999**, *84*, 329–336.
- (47) Pucadyil, T. J.; Chattopadhyay, A. Role of cholesterol in the function and organization of G protein-coupled receptors. *Prog. Lipid Res.* **2006**, *45*, 295–333.
- (48) Paila, Y. D.; Chattopadhyay, A. Membrane cholesterol in the function and organization of G-protein coupled receptors. *Subcell. Biochem.* **2010**, *51*, 439–466.
- (49) Jafurulla, M.; Chattopadhyay, A. Membrane lipids in the function of serotonin and adrenergic receptors. *Curr. Med. Chem.* **2013**, *20*, 47–55.
- (50) Sengupta, D.; Chattopadhyay, A. Molecular dynamics simulations of GPCR-cholesterol interaction: An emerging paradigm. *Biochim. Biophys. Acta* **2015**, *1848*, 1775–1782.
- (51) Sengupta, D.; Prasanna, X.; Mohole, M.; Chattopadhyay, A. Exploring GPCR-lipid interactions by molecular dynamics simulations: Excitements, challenges, and the way forward. *J. Phys. Chem. B* **2018**, *122*, 5727–5737.
- (52) Sengupta, D.; Kumar, G. A.; Prasanna, X.; Chattopadhyay, A. Experimental and Computational Approaches to Study Membranes and Lipid-Protein Interactions. In *Computational Biophysics of Membrane Proteins*; Domene, C., Ed.; Royal Society of Chemistry: London, 2017; pp 137–160.
- (53) Kumar, G. A.; Chattopadhyay, A. Statin-induced chronic cholesterol depletion switches GPCR endocytosis and trafficking: Insights from the serotonin<sub>1A</sub> receptor. *ACS Chem. Neurosci.* **2020**, *11*, 453–465.
- (54) Kumar, G. A.; Chattopadhyay, A. Membrane cholesterol regulates endocytosis and trafficking of the serotonin<sub>1A</sub> receptor: Insights from acute cholesterol depletion. *Biochim. Biophys. Acta, Mol. Cell Biol. Lipids* **2021**, *1866*, 158882.
- (55) Sharma, A.; Kumar, G. A.; Chattopadhyay, A. Late endosomal/lysosomal accumulation of a neurotransmitter receptor in a cellular model of Smith-Lemli-Opitz syndrome. *Traffic* **2021**, *22*, 332–344.
- (56) Zhao, F.; Yang, J.; Cui, R. Effect of hypoxic injury in mood disorder. *Neural Plast.* **2017**, *2017*, 6986983.
- (57) Kalipatnapu, S.; Pucadyil, T. J.; Harikumar, K. G.; Chattopadhyay, A. Ligand binding characteristics of human serotonin<sub>1A</sub> receptor heterologously expressed in CHO cells. *Biosci. Rep.* **2004**, *24*, 101–115.
- (58) Pucadyil, T. J.; Kalipatnapu, S.; Harikumar, K. G.; Rangaraj, N.; Karnik, S. S.; Chattopadhyay, A. G-protein-dependent cell surface dynamics of the human serotonin<sub>1A</sub> receptor tagged to yellow fluorescent protein. *Biochemistry* **2004**, *43*, 15852–15862.
- (59) Anderson, R. H.; Sochacki, K. A.; Vuppula, H.; Scott, B. L.; Bailey, E. M.; Schultz, M. M.; Kerkvliet, J. G.; Taraska, J. W.; Hoppe, A. D.; Francis, K. R. Sterols lower energetic barriers of membrane bending and fission necessary for efficient clathrin-mediated endocytosis. *Cell Rep.* **2021**, *37*, 110008.
- (60) Amundson, D. M.; Zhou, M. Fluorometric method for the enzymatic determination of cholesterol. *J. Biochem. Biophys. Methods* **1999**, *38*, 43–52.
- (61) Snyder, C. M.; Chandel, N. S. Mitochondrial regulation of cell survival and death during low-oxygen conditions. *Antioxid. Redox Signaling* **2009**, *11*, 2673–2683.
- (62) Stäubert, C.; Krakowsky, R.; Bhuiyan, H.; Witek, B.; Lindahl, A.; Broom, O.; Nordström, A. Increased lanosterol turnover: A metabolic burden for daunorubicin-resistant leukemia cells. *Med. Oncol.* **2016**, *33*, 6.
- (63) Bloch, K. E. Sterol structure and membrane function. *CRC Crit. Rev. Biochem.* **1983**, *14*, 47–92.
- (64) Mariño, G.; Kroemer, G. Mechanisms of apoptotic phosphatidylserine exposure. *Cell Res.* **2013**, *23*, 1247–1248.
- (65) Zhang, G.; Gurtu, V.; Kain, S. R.; Yan, G. Early detection of apoptosis using a fluorescent conjugate of Annexin V. *Biotechniques* **1997**, *23*, 525–531.
- (66) Malmberg, A.; Strange, P. G. Site-directed mutations in the third intracellular loop of the 5-HT<sub>1A</sub> receptor alter G protein coupling from G<sub>i</sub> to G<sub>s</sub> in a ligand-dependent manner. *J. Neurochem.* **2000**, *75*, 1283–1293.
- (67) Raymond, J. R.; Mukhin, Y. V.; Gettys, T. W.; Garnovskaya, M. N. The recombinant 5-HT<sub>1A</sub> receptor: G protein coupling and signalling pathways. *Br. J. Pharmacol.* **1999**, *127*, 1751–1764.
- (68) Tardieu, J.-L. Selecting a cyclic AMP kit for assaying GPCR target activation. *Nat. Methods* **2008**, *5*, iii–iv.
- (69) Ward, R. J.; Pediani, J. D.; Harikumar, K. G.; Miller, L. J.; Milligan, G. Spatial intensity distribution analysis quantifies the extent and regulation of homodimerization of the secretin receptor. *Biochem. J.* **2017**, *474*, 1879–1895.
- (70) Kumar, G. A.; Sarkar, P.; Stepniewski, T. M.; Jafurulla, M.; Singh, S. P.; Selent, J.; Chattopadhyay, A. A molecular sensor for cholesterol in the human serotonin<sub>1A</sub> receptor. *Sci. Adv.* **2021**, *7*, No. eabh2922.
- (71) Quillinan, N.; Herson, P. S.; Traystman, R. J. Neuro-pathophysiology of brain injury. *Anesthesiol. Clin.* **2016**, *34*, 453–464.
- (72) Azmitia, E. C. Serotonin and brain: Evolution, neuroplasticity, and homeostasis. *Int. Rev. Neurobiol.* **2007**, *77*, 31–56.
- (73) Štrac, D. Š.; Pivac, N.; Mück-Seler, D. The serotonergic system and cognitive function. *Transl. Neurosci.* **2016**, *7*, 35–49.
- (74) Palacios, J. M.; Waeber, C.; Hoyer, D.; Mengod, G. Distribution of serotonin receptors. *Ann. N.Y. Acad. Sci.* **1990**, *600*, 36–52.
- (75) Assad, F.; Schultheiss, R.; Leniger-Follert, E.; Wüllenweber, R. Measurement of Local Oxygen Partial Pressure (PO<sub>2</sub>) of the Brain Cortex in Cases of Brain Tumors. In *CNS Metastases Neurosurgery in the Aged*; Piotrowski, W., Brock, M., Klingler, M., Eds.; Advances in Neurosurgery; Springer: Berlin, Heidelberg, 1984; Vol. 12, pp 263–270.
- (76) Meixensberger, J.; Dings, J.; Kuhnigk, H.; Roosen, K. Studies of tissue PO<sub>2</sub> in normal and pathological human brain cortex. *Acta Neurochir. Suppl.* **1993**, *59*, 58–63.
- (77) Hoffman, W. E.; Charbel, F. T.; Edelman, G. Brain tissue oxygen, carbon dioxide, and pH in neurosurgical patients at risk for ischemia. *Anesth. Analg.* **1996**, *82*, 582–586.
- (78) Dings, J.; Meixensberger, J.; Jäger, A.; Roosen, K. Clinical experience with 118 brain tissue oxygen partial pressure catheter probes. *Neurosurgery* **1998**, *43*, 1082–1094.
- (79) Korsic, M.; Jugović, D.; Kremzar, B. Intracranial pressure and biochemical indicators of brain damage: follow-up study. *Croat. Med. J.* **2006**, *47*, 246–252.
- (80) Hussain, G.; Wang, J.; Rasul, A.; Anwar, H.; Imran, A.; Qasim, M.; Zafar, S.; Kamran, S. K. S.; Razzaq, A.; Aziz, N.; Ahmad, W.; Shabbir, A.; Iqbal, J.; Baig, S. M.; Sun, T. Role of cholesterol and sphingolipids in brain development and neurological diseases. *Lipids Health Dis.* **2019**, *18*, 26.

- (81) Zhang, J.; Liu, Q. Cholesterol metabolism and homeostasis in the brain. *Protein Cell* **2015**, *6*, 254–264.
- (82) Dietschy, J. M.; Turley, S. D. Cholesterol metabolism in the brain. *Curr. Opin. Lipidol.* **2001**, *12*, 105–112.
- (83) Björkhem, I.; Meaney, S. Brain cholesterol: Long secret life behind a barrier. *Arterioscler., Thromb., Vasc. Biol.* **2004**, *24*, 806–815.
- (84) Chattopadhyay, A.; Paila, Y. D. Lipid-protein interactions, regulation and dysfunction of brain cholesterol. *Biochem. Biophys. Res. Commun.* **2007**, *354*, 627–633.
- (85) Waterham, H. R. Defects of cholesterol biosynthesis. *FEBS Lett.* **2006**, *580*, 5442–5449.
- (86) Jafurulla, M.; Rao, B. D.; Sreedevi, S.; Ruyschaert, J.-M.; Covey, D. F.; Chattopadhyay, A. Stereospecific requirement of cholesterol in the function of the serotonin<sub>1A</sub> receptor. *Biochim. Biophys. Acta* **2014**, *1838*, 158–163.
- (87) Jafurulla, M.; Chattopadhyay, A. Structural stringency of cholesterol for membrane protein function utilizing stereoisomers as novel tools: A review. *Methods Mol. Biol.* **2017**, *1583*, 21–39.
- (88) Sarkar, P.; Jafurulla, M.; Bhowmick, S.; Chattopadhyay, A. Structural stringency and optimal nature of cholesterol requirement in the function of the serotonin<sub>1A</sub> receptor. *J. Membr. Biol.* **2020**, *253*, 445–457.
- (89) Jafurulla, M.; Aditya Kumar, G.; Rao, B. D.; Chattopadhyay, A. A critical analysis of molecular mechanisms underlying membrane cholesterol sensitivity of GPCRs. *Adv. Exp. Med. Biol.* **2019**, *1115*, 21–52.
- (90) Sarkar, P.; Chattopadhyay, A. Cholesterol interaction motifs in G protein-coupled receptors: Slippery hot spots? *Wiley Interdiscip. Rev.: Syst. Biol. Med.* **2020**, *12*, No. e1481.
- (91) Dawaliby, R.; Trubbia, C.; Delporte, C.; Noyon, C.; Ruyschaert, J.-M.; Van Antwerpen, P.; Govaerts, C. Phosphatidylethanolamine is a key regulator of membrane fluidity in eukaryotic cells. *J. Biol. Chem.* **2016**, *291*, 3658–3667.
- (92) Yu, Y.; Vidalino, L.; Anesi, A.; Macchi, P.; Guella, G. A lipidomics investigation of the induced hypoxia stress on HeLa cells by using MS and NMR techniques. *Mol. BioSyst.* **2014**, *10*, 878–890.
- (93) Revin, V.; Grunuyshkin, I.; Gromova, N.; Revina, E.; Abdulwahid, A. S. A.; Solomadin, I.; Tychkov, A.; Kukina, A.; Kukina, A. Effect of hypoxia on the composition and state of lipids and oxygen-transport properties of erythrocyte haemoglobin. *Biotechnol. Biotechnol. Equip.* **2017**, *31*, 128–137.
- (94) Adelantado, N.; Tarazona, P.; Grillitsch, K.; García-Ortega, X.; Monforte, S.; Valero, F.; Feussner, I.; Daum, G.; Ferrer, P. The effect of hypoxia on the lipidome of recombinant *Pichia pastoris*. *Microb. Cell Fact.* **2017**, *16*, 86.
- (95) O'Brien, K. A.; Atkinson, R. A.; Richardson, L.; Koulman, A.; Murray, A. J.; Harridge, S.; Martin, D. S.; Levett, D.; Mitchell, K.; Mythen, M. G.; Montgomery, H. E.; Grocott, M.; Griffin, J. L.; Edwards, L. M. Metabolomic and lipidomic plasma profile changes in human participants ascending to Everest base camp. *Sci. Rep.* **2019**, *9*, 2297.
- (96) Kious, B. M.; Kondo, D. G.; Renshaw, P. F. Living high and feeling low: Altitude, suicide, and depression. *Harv. Rev. Psychiatr.* **2018**, *26*, 43–56.
- (97) Smith, P. K.; Krohn, R. I.; Hermanson, G. T.; Mallia, A. K.; Gartner, F. H.; Provenzano, M. D.; Fujimoto, E. K.; Goeke, N. M.; Olson, B. J.; Klenk, D. C. Measurement of protein using bicinchoninic acid. *Anal. Biochem.* **1985**, *150*, 76–85.
- (98) Bligh, E. G.; Dyer, W. J. A rapid method of total lipid extraction and purification. *Can. J. Biochem.* **1959**, *37*, 911–917.
- (99) Raskin, P.; Siperstein, M. D. Mevalonate metabolism by renal tissue in vitro. *J. Lipid Res.* **1974**, *15*, 20–25.
- (100) Shrivastava, S.; Sarkar, P.; Preira, P.; Salomé, L.; Chattopadhyay, A. Role of actin cytoskeleton in dynamics and function of the serotonin<sub>1A</sub> receptor. *Biophys. J.* **2020**, *118*, 944–956.